Modified Fokker-Planck approach to steady-state distributions in plasmas

Jun Li and Yukap Hahn
Physics Department, University of Connecticut, Storrs, Connecticut 06269
(Received 22 April 1994; revised manuscript received 9 December 1994)

A diffusion-equation approach to the collisional radiative recombination and ionization processes in plasmas is improved in order to be applicable to low density plasmas. Dense excited levels are assumed to be quasicontinuous and thus treated by Fokker-Planck equations in the nearest neighbor (nn) approximation, and a few levels lying below the bottleneck are retained explicitly as a discrete set. These coupled equations are solved iteratively, which in turn allows incorporation of the corrections to the nn approximation. The method has been tested for the simple hydrogen plasma in a steady state. The numerical results agree with the exact solutions. Extensions of this approach to nonequilibrium plasmas and complex plasmas of heavy ions are discussed.

PACS number(s): 52.20.−j, 52.80.−s

I. INTRODUCTION

Many studies have been carried out in recent years to model laboratory and astrophysical plasmas which are of interesting importance in a multitude of applications [1]. Plasma parameters of interest are wide ranged, with temperatures from sub eV to tens of keV and densities from 10^3 cm^{-3} to 10^{24} cm^{-3}, where the latter corresponds to the near normal density of solids. Modeling and diagnostics of such diverse plasmas cannot be carried out by one single theory, which may be too complex and unwieldy. Approximate theories have to be carefully tailored to suit particular systems. For high-density plasmas, where either local thermodynamic equilibrium (LTE) or partial LTE prevails, several models of the rate equation approach have been successfully built, by combining a large number of states which are in LTE into one pseudo level. This greatly simplifies the system and makes the otherwise insurmountable problem solvable [2,3].

For low-density plasmas of interest in the present study, with density 10^{18} cm^{-3} or less, LTE is not a good approximation for low-lying levels, and it is often necessary to solve a large set of rate equations for these non-LTE levels. The coupled rate equations depend on the various atomic (and ionic) processes which take place inside plasmas [4]. The necessary atomic input data for the rate equations are expressed in terms of the electron-ion transition rates for collisional excitation, deexcitation and ionization, radiative decay and recombination, and related resonant processes. (In addition, ion-atom and ion-ion interactions are also important, but we do not consider them explicitly here.) The reaction rates are usually evaluated theoretically, assuming that (a) the plasma electrons and ions are in local thermal equilibrium, and (b) the plasma environment (created mainly by ions) does not affect the electronic rates themselves, in terms of its microfield distortion. Evidently, both these assumptions are only partially valid in many cases, and can seriously affect the outcome of analyses. Plasma electrons cause collisional transitions among the atomic (and ionic) levels, and this is the subject of the present study. The plasma field distortions will be treated in later reports.

The collisional transition effect of plasma electrons and radiative coupling are conventionally treated by a set of rate equations. (Collisions of the target with plasma ions, leading to charge exchange and ionization, also seem to be important but are neglected here.) The resulting steady-state solutions provide population densities of the excited states of ions, and also the effective collisional-radiative recombination and ionization rates for the ground state, i.e., α_1 and S_1, respectively. Two approaches have been developed in the past in the construction of the rate equations, where the excited states of the ions are treated either as discrete levels or as continuous. The number of states included in the first approach can be very large [5–7], often reaching many thousands of excited Rydberg states and several charge states. For ions with more than one electron, multiple excited states are present. Dynamical properties of densely populated levels are probably similar to each other. In addition, when the plasma distortions due to plasma ions are introduced, identification of these excited states is no longer possible, due to the strong field mixing of closely packed Rydberg states. The continuum approach [8–11] may therefore be more convenient for treating the closely spaced levels of mixed spectra. A proper adjustment of the input rates and their spread in energy due to field mixing [13] is necessary, but such a program is in general difficult to carry out. Nevertheless, the continuum treatment in the form of Fokker-Planck equations [8–11] may be the most effective at high densities ($> 10^{18}$ cm^{-3}) where collisional processes dominate over the radiative effects.

We examine in this paper the continuum approach to ionic state distribution developed previously [8–12] and critically assess its applicability for low-density plasmas. The study is carried out for the hydrogen model plasma, where the complications due to the presence of multicharged ions and resonant processes are absent. Our discussion focuses on weakly coupled low- and medium-density plasmas, with densities of 10^8–10^{18} cm^{-3} and temperatures in the range of 0.5–5 eV. As will be shown, the previous formulation cannot adequately describe the low-density plasmas, even in their steady state. The theory is improved here to remedy some of these difficulties. For strongly coupled plasmas of high density, the overall theories may simplify while the plasma field effect becomes more critical. The transient problem is treated in a separate report [14], where a low-density, low-temperature plasma formed by two merged beams of electrons and ions is studied as they relaxed in their relative rest frame.

II. THE RATE EQUATION APPROACH

In the hydrogen plasma model of Bates, Kingston, and McWhirter (BKM) [5], the collisional-radiative recombination of electrons with bare protons to form hydrogen atoms was discussed. The rate of change of the population density of level p at time t is given by

$$\dot{n}_p = -n_p[n_c\mathcal{K}_p + \mathcal{A}_p] + n_c \sum_{q\neq p}^{p_c} n_q K_{qp} + \sum_{q>p}^{c} p_c\, n_q A_{qp} + n_c n_I[K_{cp} + \beta_p] , \quad (1)$$

where $\mathcal{K}_p = K_{pc} + \sum_{q\neq p}^{p_c} K_{pq}$, $\mathcal{A}_p = \sum_{q<p} A_{pq}$. In (1), n_c and n_I are the population densities of free electrons and bare protons, K_{cp} is the rate coefficient for the three-body recombination process from c(continuum)$\rightarrow p$(discrete), K_{pc} is the rate coefficient for the inverse, collisional ionization process, K_{pq} is the rate coefficient for the collisional excitation or deexcitation transitions from $p \rightarrow q$, β_p is the rate coefficient for radiative recombination process $c \rightarrow p$, and A_{pq} is the spontaneous transition probability from $p \rightarrow q$, with $p > q$. We introduce a high p cutoff at $p = p_c$. This is a nontrivial modification of the original BKM model. It takes into account the collective effect of plasma electrons, as a Debye screening of the target ions, with $p_c \sim (kT/n_c)^{1/4}$ in a.u. This cutoff places an upper bound on the total number of recombined hydrogen atoms, thus making the model more realistic. The principal assumptions introduced in the construction of Eq. (1) are as follows.

(i) The continuum electron density n_c and the bare ion density n_I are held constant during the entire period of relaxation (for neutral plasmas, we also have $n_c = n_I$). This makes the model simple, but can result in unrealistically large final state populations for low-lying states, especially at low temperatures.

(ii) The distribution among the degenerate sublevels of a given principal quantum number p is assumed statistical, i.e., the angular and azimuthal quantum numbers are averaged over. This is reasonable when collisions that mix degenerate states are very rapid.

(iii) The plasma is optically thin so that all the radiation emitted during the relaxation to stationary states escapes without reabsorption. This limits the validity of the model to low and medium densities. The plasma boundary effects are also ignored.

When p is large enough, $p > p_s$ for some number p_s, collisional processes become dominant so that the population density n_p of hydrogen in the excited state p, is close to the Saha equilibrium value,

$$n_p^e = p^2[h^2/2\pi mkT]^{3/2}\exp(I_p/KT) n_c n_I , \quad (2)$$

where I_p is the ionization potential. The parameter p_s depends on the free electron density as well as temperature T. Therefore, for convenience, the population density may be normalized, i.e.,

$$P_p = n_p / n_p^e , \quad (3)$$

which then has the property that

$$P_p \approx 1, \quad p \ge p_s . \quad (4)$$

By detailed balance

$$n_q^e K_{qp} = n_p^e K_{pq}, \quad n_I K_{cp} = n_p^e K_{pc} , \quad (5)$$

and the rate equations (1) become

$$\dot{P}_p = -P_p[n_c\mathcal{K}_p + \mathcal{A}_p] + n_c \sum_{q\neq p}^{p_c} P_q K_{pq} + \sum_{q>p}^{p_c} P_q \frac{n_q^e}{n_p^e} A_{qp} + n_c K_{pc} + \frac{n_c n_I}{n_p^e}\beta_p . \quad (6)$$

Because of the property (4), (6) is effectively truncated to a finite set of p_s equations; that is, for $p_s < p, q < p_c$, we set $P_p = 1$ in (6). Generally, the excited states with large p relax much faster than the ground state in the case of hydrogen plasma. Therefore, as was done originally by Bates, Kingston, and McWhirter [5], a quasi-steady-state solution may be obtained by setting $\dot{P}_p = 0, (p \neq 1)$ in (6) and by writing P_p in the form

$$P_p = r_p^0 + r_p^1 P_1, \quad (p \neq 1) . \quad (7)$$

The parameters r_p^0 and r_p^1 are obtained by inverting a $(p_s - 1)\times(p_s - 1)$ matrix formed from a part of the right hand side of (6) for $p \neq 1$. Substitution of (7) into the equation for P_1 eliminates the quantities $P_p, p = 2, 3, \ldots$, and gives

$$\dot{P}_1 = [n_c n_I / n_1^e]\alpha_1 - n_c S_1 P_1 , \quad (8)$$

where α_1 and S_1 are the collisional-radiative recombination and ionization coefficients [5] for the ground state $p = 1$. When the system achieves a final equilibrium state, we set $\dot{P}_1 = 0$ and obtain $P_1 = [n_I / n_1^e][\alpha_1 / S_1]$. All the other population densities can then be obtained by substituting this expression for P_1 into (7).

III. A MODIFIED FOKKER-PLANCK APPROACH

A bound electron in state p undergoes level to level transitions, caused by collisions with plasma electron perturbers. It often follows a long and irregular path among the ionic energy levels before reaching the final state. This meandering path is sometimes interrupted by radiative decays. Thus the analogy between the motion of the electron in the energy level space of the atom and the "random walk" of a Brownian particle in a liquid may be exploited in formulating the plasma electron effect [12], especially when nearest-neighbor (nn) collisions dominate. Such a formulation was given earlier [8–12], but its applicability has not been thoroughly investigated. In this paper, we reexamine the theory for hydrogenic plasmas and improve the model so as to be applicable at low densities.

The dense spectrum of the upper Rydberg states of hydrogen atom is suitable for a quasicontinuum treatment, but the low-lying levels are widely spaced so that (i) the continuum treatment of these levels is a poor approximation. Furthermore, (ii) the radiative processes are nonlocal in the sense that the Markov nn approximation is a very poor approximation, and (iii) the higher states cut off by screening ($p > p_c$) must be imposed to make the model realistic. (iv) The rates are in general distorted by plasma ions so that the rates evaluated at zero density may need adjustment. (v) For low-temperature plasmas, the densities n_c and n_I may not be constant in the steady-state limit because of the electron capture.

Based on these considerations, we treat here the problems (i)–(iii) by separating several low-lying levels from the closely packed upper levels, and apply the continuum treatment for the upper levels. That is, we have $1 \le p \le p_b$ for the discrete levels and $p_b < p < p_c$ for the continuum, where p_b is the bottleneck p. This separation requires an iterative procedure between the discrete and continuum parts. Determination of p_b is based on the condition to be described below, and it usually assumes the value $p_b \sim 2-4$ in the hydrogen plasma for the densities considered here, and increases with decreasing density. In practice of course this value is not known *a priori*, and we simply take a value, say $p_b \approx 4$. The final result should be insensitive to this if p_b is chosen large enough. The separation and subsequent iterative procedure rectifies the difficulties (i)–(iii) and is the main departure of our approach from the earlier formulation. In particular, this allows inclusion of the corrections to Markov approximation. The difficulties (iv) and (v) are treated in separate reports [14,15].

We summarize here the main steps involved. We define

$$R_{pq} = \begin{cases} n_c K_{qp} + \dfrac{n_p^e}{n_q^e} A_{pq} & (p > q) , \\ -(n_c \mathcal{K}_q + \mathcal{A}_q) & (p = q) , \\ n_c K_{qp} & (p < q) ; \end{cases} \tag{9}$$

and

$$R_{cp} = n_c K_{pc} + \frac{n_c n_I}{n_p^e} \beta_p . \tag{10}$$

For the present case, the first four levels are taken to be discrete and coupled to upper levels which are converted to a simple quasicontinuum. For equilibrium, the rate equations assume the form

$$\frac{\partial P_p}{\partial t} = \sum_{q=1}^{4} R_{qp} P_q + \sum_{q=5}^{p_c} R_{qp} Y(E_q) + R_{cp} = 0 \quad (p = 1,2,3,4) ; \tag{11}$$

$$\begin{aligned} \frac{\partial Y(E_p)}{\partial t} = {} & \sum_{q=1}^{4} R_{qp} P_q + \sum_{q=5}^{p-2} R_{qp} Y(E_q) + R_{(p-1)p} Y(E_{p-1}) \\ & + R_{pp} Y(E_p) + R_{(p+1)p} Y(E_{p+1}) \\ & + \sum_{q=p+2}^{p_c} R_{qp} Y(E_q) + R_{cp} = 0, \quad (p > 4) , \end{aligned} \tag{12}$$

where $Y(E_p)$ is the normalized electronic population density $Y = P_p$ for $p > 4$, with the variable change $E_p = -1/p^2$ Ry. As E_p ($p > 4$) is a continuous variable, a Taylor expansion of the population density to second order is used, i.e.,

$$\begin{aligned} Y(E_{p\pm1}) = {} & Y(E_p) + (E_{p\pm1} - E_p) Y'(E_p) \\ & + \tfrac{1}{2}(E_{p\pm1} - E_p)^2 Y''(E_p) . \end{aligned}$$

The rate Eqs. (11) and (12) then become,

$$\frac{\partial P_p}{\partial t} = \sum_{q=1}^{4} R_{qp} P_q + \int_{E_4^+}^{E_c} R_{E_p} Y(E) dE + R_{cp} = 0 \quad (p = 1,2,3,4) , \tag{13}$$

$$\frac{\partial Y(E,t)}{\partial t} = B_2 \frac{\partial^2 Y(E)}{\partial E^2} + B_1 \frac{\partial Y(E)}{\partial E} + B_0 Y(E) + B_{-1} = 0 \quad (E > E_4^+) , \tag{14}$$

where

$$\begin{aligned} & E_c = -1/p_c^2 \\ & B_2 = \tfrac{1}{2} R_{(p-1)p} (E_{p-1} - E_p)^2 + \tfrac{1}{2} R_{(p+1)p} (E_{p+1} - E_p)^2 , \\ & B_1 = R_{(p-1)p} (E_{p-1} - E_p) + R_{(p+1)p} (E_{p+1} - E_p) , \\ & B_0 = R_{(p+1)p} + R_{pp} + R_{(p-1)p} , \\ & B_{-1} = \sum_{q=1}^{4} R_{qE} P_q + \int_{E_4^+}^{E_{p-2}^+} R_{E'E} Y(E') dE' \\ & \qquad + \int_{E_{p+1}^+}^{E_c} R_{E'E} Y(E') dE' + R_{cp} , \end{aligned} \tag{15}$$

and $E_p^+ = E_p + \delta_p, \delta_p \approx \frac{1}{2}(E_{p+1} - E_p)$. Equation (14) is the desired Fokker-Planck equation. Note that the non-Markovian terms ($p' \ne p \pm 1, p$) are included in B_{-1} and in the two integral terms in (15); they are found to be very important at low densities and treated through the iteration cycles. Incidentally, if we eliminate the explicit E dependence of Y by averaging all the quantities in Eq. (14) over E, the resulting model is simple and similar to that of Ref. [3]. In fact, the two- and three-level models introduced earlier in Ref. [7] are equivalent to such an approximation. These models can readily be generalized to plasmas with multiple charge states.

The boundary conditions are

$$Y(E_4^+) = P_{4^+}, \quad \text{and} \quad Y(E_c) = 1 ,$$

where P_{4^+} is obtained by extrapolation from below ($p \le 4$). Equations (13) and (14) are solved by iteration. To order $(\partial^3 Y / \partial E)(\Delta E)^3$, the resulting solution is

$$Y(E)=U^{-1}(E)[C_1+C_2V(E)-F(E)] , \tag{16}$$

where

$$\begin{aligned}
U(E)&=\int_{E_4^+}^{E^+}\frac{B_1(\tilde E)-B_2'(\tilde E)}{B_2(\tilde E)}d\tilde E ,\\
V(E)&=\int_{E_4^+}^{E^+}\frac{U(\tilde E)}{B_2(\tilde E)}d\tilde E ,\\
F(E)&=\int_{E_4^+}^{E^+}\frac{U(\tilde E)f(\tilde E)}{B_2(\tilde E)}d\tilde E ,\\
f(E)&=\int_{E_4^+}^{E^+}\{B_{-1}(\tilde E)+Y(\tilde E)[B_0(\tilde E)-B_1'(\tilde E)\\
&\qquad -B_2''(\tilde E)]\}d\tilde E ,
\end{aligned} \tag{17}$$

and $E^+\approx E+\delta E$, where $\delta E=\Delta p\partial E/\partial p=|E|^{3/2}$ for $E=-1/p^2$ (Ry). This is valid for $E>E_b$. The constants C_1 and C_2 are determined by the boundary conditions, to be

$$C_1=P_{4^+}, \text{ and } C_2=V^{-1}(E_c)[U(E_c)+F(E_c)-P_{4^+}] .$$

The magnitudes of the coefficients B_2, B_1, B_0, and B_{-1} in Eq. (14) are often such that B_2 and B_1 are small in magnitude compared to B_0 and B_{-1}, and $B_0\approx -B_{-1}$, thus causing a large cancellation for high-lying levels when $Y\approx 1$. This can sometimes make the solution numerically unstable. The momentum variable has also been tried in place of E, but the instability is still present in some cases, especially at low densities. For the actual calculation, we have therefore adopted p as the variable which is continuous for $p>4$, and have obtained the following rate equations from (11) and (12):

$$\frac{\partial P_p}{\partial t}=\sum_{q=1}^{4}R_{qp}P_q+\int_{4^+}^{p_c}R_{qp}Y(q)dq+R_{cp}=0; \qquad p=1,2,3,4 , \tag{18}$$

$$\frac{\partial Y(p,t)}{\partial t}=D_2\frac{\partial^2 Y(p)}{\partial p^2}+D_1\frac{\partial Y(p)}{\partial p}+D_0Y(p)+D_{-1}=0; \qquad p>4 . \tag{19}$$

In (18) and (19), we have introduced the quantities

$$\begin{aligned}
D_2&=\tfrac{1}{2}(R_{(p-1)p}+R_{(p+1)p}) ,\\
D_1&=-R_{(p-1)p}+R_{(p+1)p} ,\\
D_0&=R_{(p+1)p}+R_{pp}+R_{(p-1)p} ,\\
D_{-1}&=\sum_{q=1}^{4}R_{qp}P_q+\int_{4^+}^{(p-2)^+}R_{qp}Y(q)dq\\
&\quad+\int_{(p+1)^+}^{p_c}R_{qp}Y(q)dq+R_{cp} ,
\end{aligned} \tag{20}$$

with $p^+\approx p+0.5$. A slight improvement in the determination of the end points in the integrals can be made using the Euler-Maclaurin formula. Equations (18) and (19) are solved in the same way as (13) and (14).

The B coefficients in (15) are related to the D coefficients in (20) by

$$\begin{aligned}
B_2&\approx D_2\left[\frac{\partial E}{\partial p}\right]^2 ,\\
B_1&\approx D_1\left[\frac{\partial E}{\partial p}\right]+D_2\left[\frac{\partial^2 E}{\partial p^2}\right] ,\\
B_0&=D_0 .\\
B_{-1}&=D_{-1} .
\end{aligned} \tag{21}$$

IV. NUMERICAL RESULTS AND DISCUSSION

We have studied the steady-state solution of the modified Fokker-Planck rate equations (14) and (19) for the hydrogen plasma. As the equations are coupled to the low-lying discrete levels by (13) and (18), we have solved them by an iterative procedure and obtained the equilibrium distribution $P_p, 1\le p\le 4$, and $Y(p)(p>4)$, for $t\to\infty$. The transient solutions of these equations will be studied in a separate report [14]. The nearest-neighbor approximation adopted in the second-order Fokker-Planck equation is in general valid when the higher derivatives and the radiative processes are negligible. That is, the Markov approximation relies on the dominance of the collisional processes represented by K_{pq}, for $q=p\pm 1$, over the radiative processes for the upper energy levels contained in $Y(p)$. But for plasmas of interest here, this is a poor approximation. On the other hand, the iterative solution includes the correction to the Markov approximation to all orders.

(1) The population density distribution. In Fig. 1, we

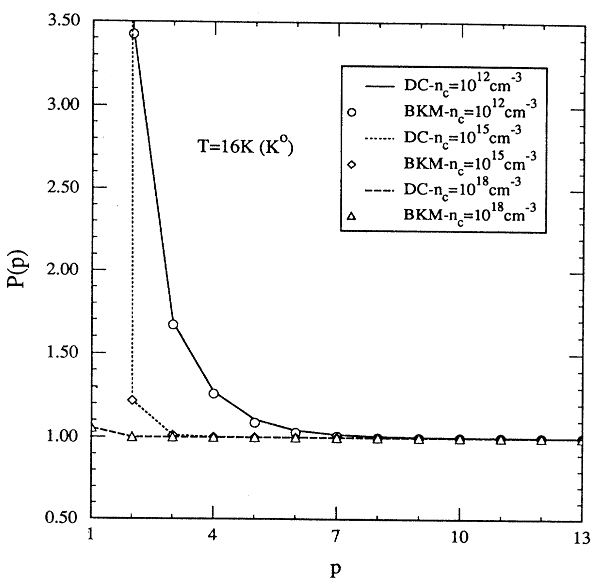

FIG. 1. The normalized steady-state population distributions P_p (and $Y=P_p$ for $p>p_b=4$) are given for three different densities $n_c=10^{12}$ (solid line), $n_c=10^{15}$ (dotted line), and $n_c=10^{18}$ (dashed line) cm^{-3}, and $T=16\,000$ K. They are calculated from the discrete-continuum (DC) Eqs. (18) and (19). The results are compared with those from the discrete BKM model (represented by circles, diamonds, and triangles). We note that the data points for $p\le p_b=4$ are treated as discrete in the theory.

show the normalized population distributions, $P_p, 1 \le p \le 4$, and $Y(p) \equiv P_p, p > 4$, for three typical cases, $n_c = 10^{12}, 10^{14}$, and 10^{18} cm^{-3}, for $T = 16\,000$ K, and compare them with those from the full BKM model. The function P increases rapidly with decreasing p, but Y approaches unity gradually with increasing p for $p > 4$. This is the "bottleneck" behavior, where

$$\left.\frac{\partial n_p}{\partial p}\right|_{p=p_b} = 0 . \tag{22}$$

It is clear from Fig. 1 that p_b increases with decreasing n_c. The choice $p_b \cong 4$ is more than adequate for the two higher densities shown, and only marginal for the case $n_c = 10^{12}$ cm^{-3}. Therefore, in practice, choosing an initial p_b (say, $p_b \cong 6$, for example) will give the correct solutions P and Y, which then reveal the optimum p_b. But the solution is rather insensitive to the initial choice of p_b, as long as it is large enough.

(2) The separation of levels into two groups, discrete and continuous. In order to illustrate the advantage of an iterative procedure where all the corrections to the Markov approximation are included, we present in Table I the collisional-radiative recombination and ionization coefficients for the ground state α_1 and S_1, respectively, which are obtained in the Markov approximation (applied only to the collisional excitation and deexcitation processes), and compare them with the exact BKM model results. This is a milder form of the nn approximation since all the radiative processes contained in the BKM model are still retained. When all the energy levels are treated with this approximation, the coefficients $\alpha_1^{\rm nn}$ and $S_1^{\rm nn}$ deviate greatly from the exact rates α_1^B and S_1^B of BKM model, especially at medium densities where the collisional excitation and deexcitation processes dominate. On the other hand, when the lowest four levels are treated separately from the continuum part, we obtain the results $\alpha_1^{\rm NN}$ and $S_1^{\rm NN}$ which are nearly exact.

(3) Stability of the Fokker-Planck rate equation. In Table II, we list the coefficients D_2, D_1, D_0, and D_{-1} of the Fokker-Planck rate equation at $T = 16\,000$ K and $n_c = 10^{15}$ cm^{-3}. When $Y \approx 1$, $(D_0 Y + D_{-1})$ shows a severe cancellation at large $p, p > 7$. Such cancellation is of course expected from (19) when $Y'(p)$ and $Y''(p)$ are small. At higher densities, this cancellation becomes more severe, which suggests that the bottleneck parameter p_b may be further reduced. The explicit calculation supports this.

In the case of the Fokker-Planck equation (14) of the variable E, the scaling factor dE/dp reduces the coefficients of the derivative terms by more than two orders of magnitude, as is evident from (21). This results in much large $Y'(E)$ and $Y''(E)$ than those in the p variable, and makes the numerical calculation less stable. Thus, although the Fokker-Planck equation in the variable E, Eq. (14), is formally equivalent to that of the variable p, Eq. (18), the latter is preferred in practice at low densities. The instability of the Fokker-Planck equation is also present with the momentum variable $k = 1/p$, even though the situation is somewhat better than the case with the variable E. For steady-state solutions, adjustment of p_b and setting $Y = 1$ in the non-Markovian terms gives reasonably good convergence.

TABLE I. The rates α_1 and S_1, defined in Eq. (8) and obtained in the nearest-neighbor (nn) approximation (for K_{pq}s only), are compared with the exact results (B) for different temperatures and densities. The nn approximation neglects all the K_{pq} with $q \neq p \pm 1$ in Eq. (1). The entry (NN) denotes the case in which the lowest four states are treated exactly as discrete levels, but the states with $p > p_b$ are treated as in the nn approximation and p continuous. The numbers in brackets denote multiplicative powers of ten.

n_c (cm^{-3})	T (K)	α_1^B (cm^{-3}/s)	$\alpha_1^{\rm NN}$ (cm^{-3}/s)	$\alpha_1^{\rm nn}$ (cm^{-3}/s)	S_1^B (cm^{-3}/s)	$S_1^{\rm NN}$ (cm^{-3}/s)	$S_1^{\rm nn}$ (cm^{-3}/s)
1.0[8]	4.0[3]	9.7[−13]	9.4[−13]	9.4[−13]	1.6[−26]	1.5[−26]	1.9[−26]
1.0[14]	4.0[3]	5.2[−11]	5.0[−11]	4.3[−11]	2.2[−24]	2.1[−24]	6.1[−25]
1.0[18]	4.0[3]	1.9[−7]	1.9[−7]	1.7[−7]	7.9[−22]	7.9[−22]	7.0[−22]
1.0[8]	8.0[3]	5.3[−13]	5.3[−13]	5.3[−13]	1.1[−17]	1.0[−17]	9.64[−18]
1.0[14]	8.0[3]	5.2[−12]	5.2[−12]	4.6[−12]	2.3[−16]	2.3[−16]	7.0[−17]
1.0[18]	8.04[3]	2.5[−9]	2.5[−9]	2.4[−9]	1.1[−14]	1.1[−14]	1.0[−14]
1.0[8]	1.6[4]	3.1[−13]	3.0[−13]	3.0[−13]	3.6[−13]	3.6[−13]	3.4[−13]
1.0[14]	1.6[4]	1.0[−12]	1.0[−12]	9.4[−13]	2.5[−12]	2.5[−12]	9.2[−13]
1.0[18]	1.6[4]	9.7[−11]	9.7[−11]	8.9[−11]	2.3[−11]	2.3[−11]	2.1[−11]
1.0[8]	3.2[4]	1.8[−13]	1.8[−13]	1.8[−13]	8.5[−11]	8.5[−11]	8.2[−11]
1.0[14]	3.2[4]	3.2[−13]	3.2[−13]	3.1[−13]	2.9[−10]	2.9[−10]	1.4[−10]
1.0[18]	3.2[4]	1.2[−11]	1.2[−11]	1.0[11]	1.1[−9]	1.1[−9]	9.6[−10]
1.0[8]	6.4[4]	1.0[−13]	1.0[−13]	1.0[−13]	1.6[−9]	1.6[−9]	1.5[−9]
1.0[14]	6.4[4]	1.3[−13]	1.3[−13]	1.3[−13]	3.6[−9]	3.6[−9]	2.1[−9]
1.0[18]	6.4[4]	2.9[−12]	2.9[−12]	2.4[−12]	8.8[−9]	8.8[−9]	7.3[−9]

TABLE II. The coefficients D_2, D_1, D_0, and D_{-1} of the Fokker-Planck equation in the variable p are given in units of $\sec^{-1}$, and at $T=16\,000$ K and $n_c=10^{12}$ cm^{-3}.

p	D_2	D_1	D_0	D_{-1}
5	2.511[7]	2.961[7]	−2.523[7]	2.809[7]
6	6.055[7]	6.060[7]	−3.904[7]	4.042[7]
7	1.262[8]	1.097[8]	−7.015[7]	7.119[7]
8	2.351[8]	1.801[8]	−1.218[8]	1.226[8]
9	4.030[8]	2.754[8]	−1.996[8]	2.003[8]
10	6.477[8]	3.990[8]	−3.105[8]	3.111[8]
11	9.894[8]	5.543[8]	−4.625[8]	4.628[8]
12	1.450[9]	7.446[8]	−6.645[8]	6.647[8]
13	2.056[9]	9.734[8]	−9.264[8]	9.264[8]

V. CONCLUSION

In this paper, a discrete-continuum Fokker-Planck approach to rate equations for modeling plasmas at low densities has been presented, where the discrete and continuum parts are separated at $p=p_b$. This has improved the reliability of the theory, where the effect of higher derivative terms and the non-Markovian corrections is minimized. By contrast, the previous formulation [8–12] in which the entire equations are in a continuum form (19) gives poor results, because the Markov approximation breaks down for low-density plasmas, and for $p<p_b$. Since the coupled set (18) and (19) requires iterative solution, the residual contributions neglected in the previous treatment can be naturally incorporated without additional complications. Thus (18) and (19) are exact to the order of $\partial^2 Y/\partial p^3$. By definition of p_b, the higher derivative terms for states with $p>p_b$ are small.

The numerical study in the case of the hydrogen plasma has shown that in general the variable p is somewhat more convenient in practice than E or the momentum, although they are formally equivalent. We have found that the discrete-continuum treatment is especially effective for low-density and low-temperature plasmas, where the Markov approximation is poor and radiative effects are important.

The theory has been tested here for a steady state, but is expected to be as effective for the time-dependent problem [14]. The main reason for this is that the high-Rydberg states contained in $Y(E)$ have relaxation time constants that are very small and similar to each other, but they are quite distinct from those for the low-lying states. Therefore, it is convenient to treat the upper states as a continuum and apply the Fokker-Planck approach.

The improved approach presented here is also applicable to treating complex plasma systems where a large number of upper levels are mixed by fields and are multiply excited, and where different charge states are present. A set of Y's corresponding to different charge states is then introduced, and the low-lying levels of each charge state are treated separately. On the other hand, for high-density plasmas, the simpler approaches of Refs. [2] and [3] may be suitable. In fact, the model described by Eqs. (18) and (19) approaches that of Ref. [3] at high density because p_c decreases to the lowest unoccupied orbitals. Furthermore, the earlier two-level and three-level models [7] were effective at high densities and are similar to Busquet's mixed model. Extensions of the present study to include multiple continua for each specific set of quantum numbers L,S,J, and to different charge states should be straightforward. Each charge state requires an additional population function Y, but considerable simplification can be achieved by "averaging" over some of the individual channels, as in Ref. [3]. For example, at a given temperature, effectively only a small number of charge states are populated, so that the rest of the charge states may be suitably averaged over.

ACKNOWLEDGMENT

This work was partially supported by a grant from the Fundamental Interactions Branch, Division of Chemical Sciences, Office of Energy Research, U.S. Department of Energy.

[1] For recent studies of dense plasmas, see, for example, *Proceedings of the Yamada Conference XXIV on Strongly Coupled Plasma Physics, Lake Yamanaka, Japan, August, 1989*, and *Proceedings of the Fifth International Workshop on Radiative Properties of Hot Dense Matter, Santa Barbara, November, 1992* [J. Quant. Spectrosc. Radiat. Transfer **51**, 1 (1994)].
[2] E. Minguez, S. Eliezer, and R. Falquina, *Proceedings of the Fifth International Workshop on Radiative Properties of Hot Dense Matter, Santa Barbara, November, 1992* [J. Quant. Spectrosc. Radiat. Transfer **51**, 229 (1994)].
[3] M. Busquet, Phys. Rev. A **25**, 2302 (1982).
[4] Y. Hahn, in *Recombination of Atomic Ions*, Vol. 296 of *NATO Advanced Study Institute, Series B: Physics*, edited by W. Graham *et al.* (Plenum, New York, 1992), p. 11.
[5] D. R. Bates, A. E. Kingston, and R. W. P. McWhirter, Proc. R. Soc. London Ser. A **267**, 297 (1962).
[6] T. Fujimoto and R. W. P. McWhirter, Phys. Rev. A **42**, 6588 (1990).
[7] J. Li and Y. Hahn, Phys. Rev. E **48**, 2934 (1993).
[8] L. P. Pitaevski, Zh. Eksp. Teor. Fiz. **42**, 1326 (1962) [Sov. Phys. JETP **15**, 919 (1962)].
[9] A. V. Gurevich and L. P. Pitaevski, Zh. Eksp. Teor. Fiz. **46**, 1281 (1964) [Sov. Phys. JETP **19**, 870 (1964)].
[10] V. S. Vorob'ev, Zh. Eksp. Teor. Fiz. **51**, 327 (1966) [Sov. Phys. JETP **24**, 218 (1967)].
[11] L. M. Biberman, V. S. Vorob'ev, and I. T. Yakubov, Teplofiz. Vys. Temp. **5**, 201 (1967) [High Temp. (USSR) **5**, 177 (1967)].
[12] L. M. Biberman, V. S. Vorob'ev, and I. T. Yakubov, *Kinetics of Nonequilibrium Low-Temperature Plasmas* (Consultant Bureau, New York, 1987).
[13] P. Krstic and Y. Hahn, Phys. Lett. A **192**, 47 (1994).
[14] J. Li and Y. Hahn (unpublished).
[15] J. Li and Y. Hahn (unpublished).